Supplementary Data for

Label-free Analysis of Breast Tissue Polarity by Raman Imaging of Lipid Phase

Shuhua Yue, Juan Manuel Cárdenas-Mora, Lesley S. Chaboub,

Sophie A. Lelièvre, Ji-Xin Cheng

Supplementary Materials and Methods:

3D culture of human mammary acini

Non-neoplastic human mammary epithelial HMT-3522 S1 cells were cultured at 37 ℃ in 5% CO_2, in chemically defined H14 medium (*Ref.* 32). H14 medium consists of DMEM/F12 (Gibco/BRL, St Louis, MO) with 250 ng/ml insulin (Boehringer Mannheim, Indianapolis, IN), 10 μg/ml transferrin (Sigma, St Louis, MO), 2.6 ng/ml sodium selenite (BD Biosciences, Bedford, MA), 10^{-10} M estradiol (Sigma), 1.4 μM hydrocortisone (BD Biosciences), 5 μg/ml luteotropic hormone (Sigma), and 10 ng/ml epidermal growth factor (EGF; BD Biosciences). H14 medium was routinely changed every 2-3 days. The high-throughput 3D culture was previously described (*Ref.* 32). Briefly cells were plated at a density of 41,520 cells / cm^2 in half the volume of medium for each 35 mm glass bottom dish. The other half of the medium containing 10% EHS material from Matrigel™ (BD Biosciences) was dripped on top of cells 5 min after cell seeding. The culture medium was changed every two to three days with EGF omitted after day 7. Acinar morphogenesis is routinely observed by day 8 to 10. The same H14 medium was used throughout the treatments with different modulators of apical polarity.

Immunostaining

Cells were permeabilized with 0.5% Triton X-100 (Sigma) for 15 min in cytoskeleton buffer [100 mM NaCl, 300 mM Sucrose, 10 mM Pipes pH 6.8, 5 mM $MgCl_2$, 1 mM pefabloc, 10 μg/ml aprotinin, 250 μM NaF], then fixed in 10% formalin (Sigma) for 20 minutes at room temperature. Antibodies against ZO-1 (Invitrogen, Carlsbad, CA, catalog # 339100; 5 μg/ml final concentration), ZO-2 (Invitrogen # 37-4700, 10 μg/ml final concentration), and hScrib (Santa Cruz, Santa Cruz, CA, catalog # SC-55543, 5 μg/ml final concentration) were used. Alexa Fluor 488 phalloidin (Molecular Probes, Eugene, OR, 5 units/ml final concentration) was used to image polymerized actin. Nuclei were stained with 4', 6-diamino-2-phenylindole (DAPI; 0.5 μg/ml) and samples were mounted in ProLong antifade solution (Molecular Probes) and stored at -20 ℃ until use.

Compound Raman microscopy and spectrum analysis

A compound Raman microscope, which integrates CARS and confocal Raman microspectroscopy on the same platform, was used for label-free analysis of apical polarity. In our apparatus, two synchronized 5-ps, 80 MHz laser oscilators (Tsunami, Spectra-Physics Lasers Inc., Mountain View, CA) are temporally synchronized and collinearly combined into a laser-scanning inverted microscope (FV300+IX71, Olympus Inc., Central Valley, PA). Pump and Stokes lasers were tuned to 707 nm (14140 cm^{-1}) and 885 nm (11300 cm^{-1}), respectively, to be in resonance with the CH_2 symmetric stretch vibration at 2840 cm^{-1}. Combined beams were focused into the specimen through a 60x water immersion objective with a 1.2 numerical aperture (UPlanApo/IR, Olympus Inc.). The forward CARS signal was collected by an air condenser with a 0.55 numerical aperture, transmitted through a 600/65 nm bandpass filter, and detected by a photomultiplier tube (PMT, H7422-40, Hamamatsu, Hamamatsu, Japan). Average acquisition time for a 512 x 512 pixels CARS image was 1.12 second, and the combined Stokes and pump

laser power at the specimen was kept constant at 40 mW. Following CARS imaging, the Stokes beam was blocked and the pump laser induced Raman scattering signal was directed toward the spectrometer (Shamrock SR-303i-A, Andor Technology, Belfast, U.K.), which was mounted to the side port of the microscope, to permit spectral analysis from 900 cm^{-1} to 3100 cm^{-1}. The spectrometer pinhole was 50-μm in diameter, which provides an axial resolution of about 4 μm. The lateral resolution was about 0.4 μm. Each Raman spectrum was acquired in 10 seconds, and pump laser power at the specimen was maintained at 15 mW. No tissue damage was observed.

For Raman analysis, two spectra were taken, one from the cell (membrane, cytoplasm, or nucleus) and the other from the glass. The glass contribution was removed by first scaling the glass profile to make its intensity of the peak-free region (2000-2600 cm^{-1}) the same as that of the cell profile, and then subtracting this modified glass profile from the cell profile. The fluorescence background in the resultant Raman spectrum was fitted by a 4^{th} order polynomial function and further removed. The 4^{th} order polynomial fit was achieved by choosing six points in the spectrum lacking any spectral features.

To determine the location of the basal and apical membrane, we first adjusted the focus to the equatorial plane of an acinus based on the CARS image (see **Fig. 1A**). We then zoomed into the apical site of the acinus by CARS (see **Fig. 1B**) and positioned the laser focus for Raman measurement on the most apical pole of certain epithelial cells in the acinus (e.g. the location indicated by the magenta circle in **Fig. 1B**). We then moved the focus to the basal site of the acinus (see **Fig. 1C**) and positioned the focus for Raman measurement on any location on the basal membrane of certain epithelial cells of the acinus (e.g. the location indicated by the blue circle in **Fig. 1C**).

Supplementary tables:

Table S1. Curve fitting parameters. The parameters of the seven Lorentzian bands used to fit the 2770 – 3070 cm^{-1} regions of all Raman spectra.

Peak center (Ω_j, cm^{-1})	Peak width (Γ_j, cm^{-1})
2845-2855	13.5
2856.5-2870	23.0
2875-2888	22.0
2885-2910	32.0
2930-2945	47.0
2958-2972	30.0
2980-3000	32.0

Table S2. Assignments of Raman peaks.

Raman peaks (cm^{-1})	Assignments	
	Protein	Lipid
2850		symmetric CH_2 stretching vibration
2860		Fermi resonance between the asymmetric CH_2 stretching mode
2882		asymmetric CH_2 stretching vibration
2902	symmetric CH_2 stretching vibrations	Fermi resonance between the asymmetric CH_2 stretching mode
2936	asymmetric CH_3 stretching vibration	symmetric CH_3 stretching vibration
2967		asymmetric CH_3 stretching vibration
2986	asymmetric CH_3 stretching vibrations	asymmetric CH_3 stretching vibration

Table S3. An example of fitted curve parameters (peak center, peak width, and area under peak) and statistics (reduced Chi-square and adj. R-square). The statistics reflect the goodness of fit. The numbers in parentheses are the corresponding standard deviations.

Peak center (Ω_j, cm^{-1})	Peak width (Γ_j, cm^{-1})	Area under peak (a.u.)	Statistics	
2855.0 (1.4)	13.5	3.3 (1.0)	Reduced Chi-Square	8.6E-4
2866.9 (3.0)	23.0	6.5 (1.2)		
2884.4 (1.7)	22.0	10.0 (1.7)		
2900.1 (2.1)	32.0	16.3 (1.9)		
2935.4 (0.9)	47.0	62.0 (1.8)	Adj. R-Square	0.992
2960.0 (2.2)	30.0	9.7 (1.6)		
2986.5 (1.3)	32.0	11.6 (0.9)		

Supplementary figures:

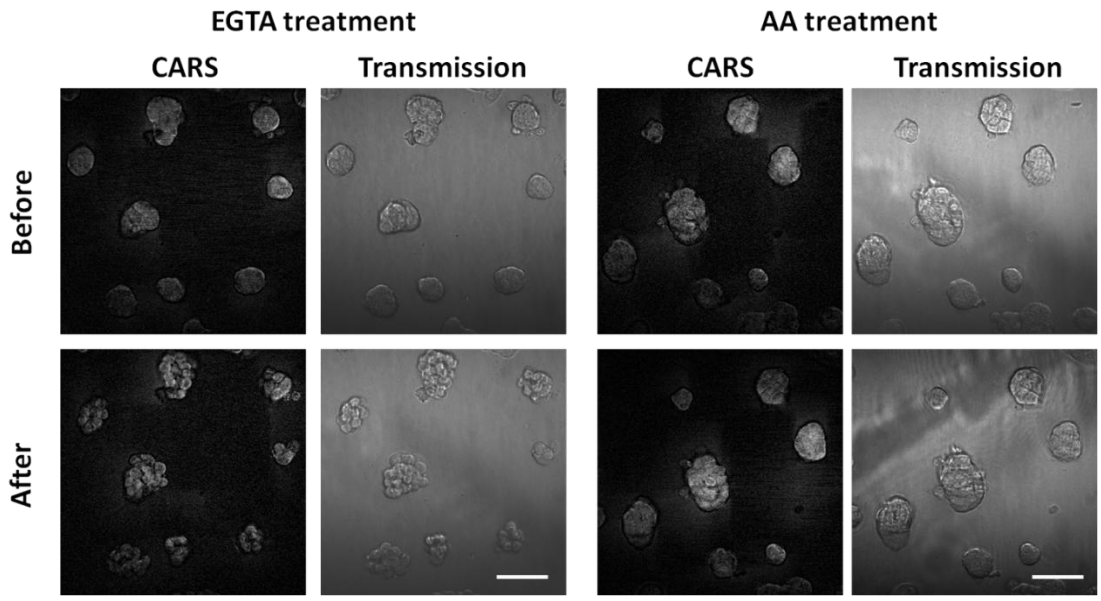

Figure S1. Longitudinal tracking of acini undergoing treatments to disrupt apical polarity. Acini were grown on gridded glass bottom culture dishes for 10 days using the high throughput method. They were located by CARS and transmission microscopy imaging before and after treatment with either EGTA or AA. Scale bars, 50 μm.

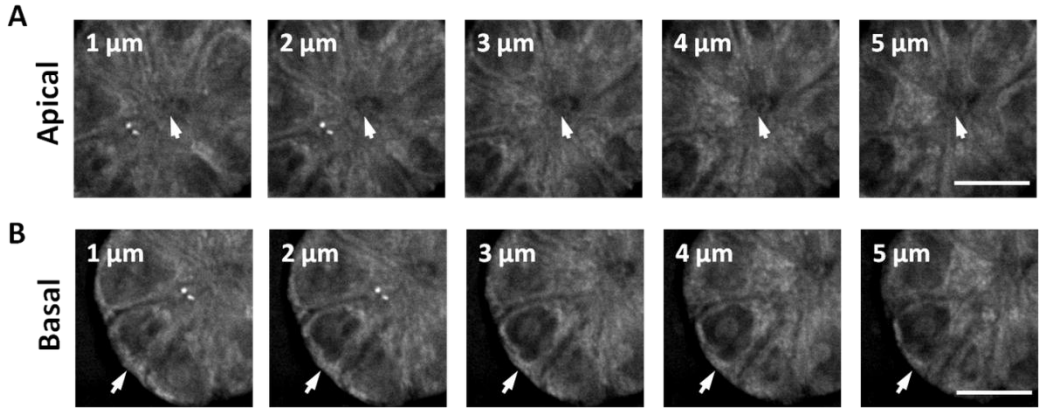

Figure S2. Depth-resolved CARS images of the apical and basal poles of a mammary acinus. Arrowheads indicate the ApM in **A** and BaM in **B**. Scale bars, 10 μm

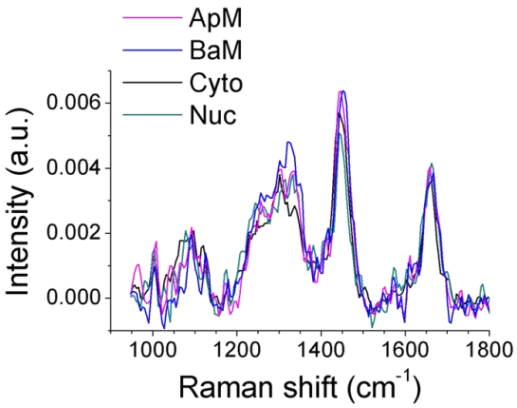

Figure S3. Raman spectra (900 – 1800 cm^{-1}) of apical membrane, basal membrane, cytoplasm, and nucleus of the acinus shown in Fig. 1A.

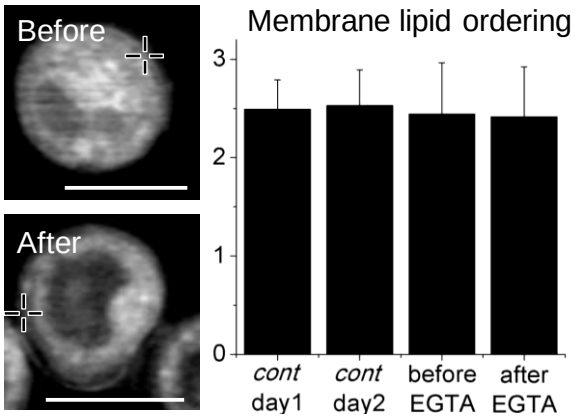

Figure S4. CARS images and membrane lipid ordering (R) of S1 cells in 3D culture before apical polarity has formed. EGTA was added on day 1 of 3D culture. Analysis was performed before and after 24h EGTA treatment. Control dishes were analyzed at the same time points. n = 5 cells. No statistical difference was found among the four compared groups (one-way ANOVA). Crosses indicate the locations for Raman spectral analysis. Scale bars, 10 μm

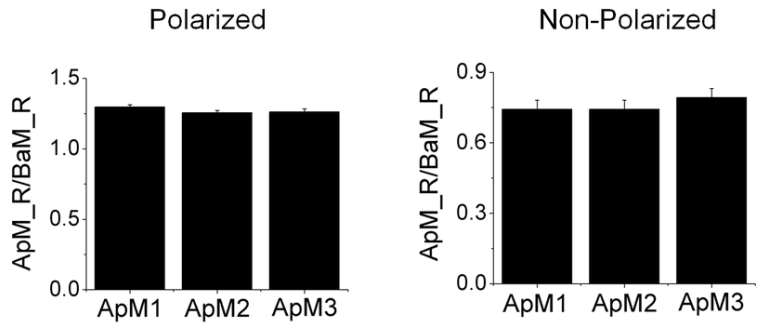

Figure S5. Reproducibility of ApM_R/BaM_R measurement. For both *P* and Non- *P* acini, ApM_R/BaM_R ratios were obtained based on three Raman scans performed at three different locations (labeled as ApM1, ApM2, ApM3) of apical membranes. No statistical significance was found using ANOVA test.

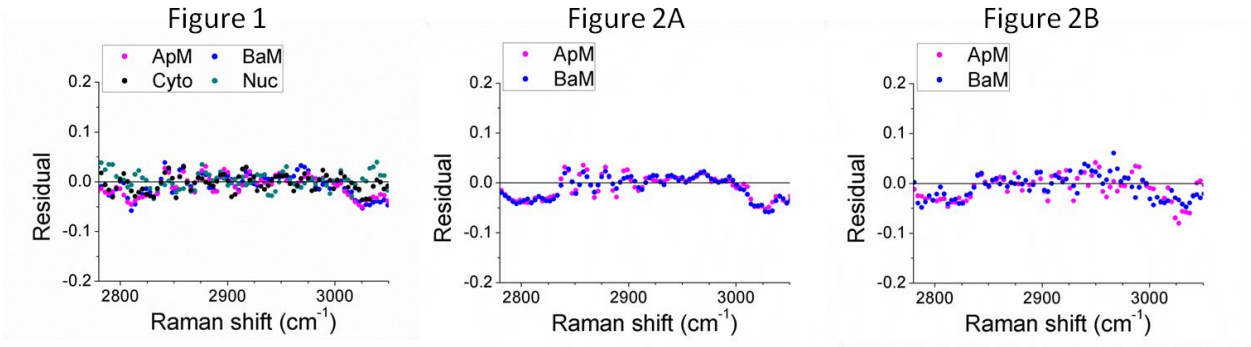

Figure S6. Residuals of the Lorentzian fittings for Fig. 1 and Fig. 2A-B.

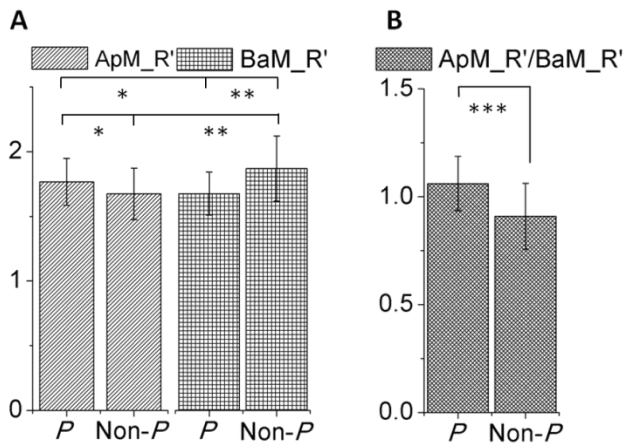

Figure S7. **Distinction between Apical membrane (ApM) and basal membrane (BaM) in polarized (*P*) and nonpolarized (Non-*P*) acini, using the ratios I_{2885}/I_{2850} (R') and ApM_R'/BaM_R'**. (A) Comparison of the ratio I_{2885}/I_{2850} (R') in ApM and BaM for both *P* mammary acini and Non-*P* mammary acini. (B) Comparison of the ratio ApM_R'/BaM_R' in *P* mammary acini and Non-*P* mammary acini. (Student's t-test, * $p < 0.05$, ** $p <$ 5.0E-4, *** $p =$ 6.1E-6, n=40 acini)

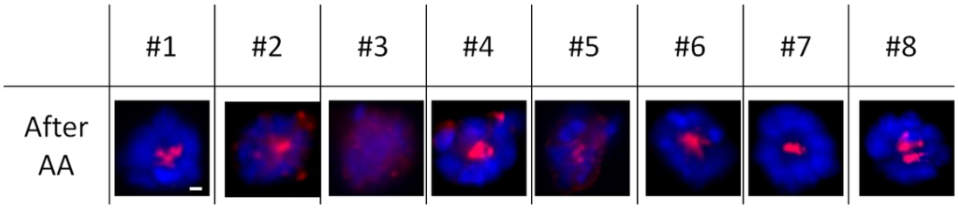

Figure S8. Immunofluorescence images of AA-treated mammary acini. Immunostaining for ZO-1 (red) and labeling for DNA (DAPI, blue) in acini following treatment with AA shown in **Fig. 5A**. Scale bar, 5 μm

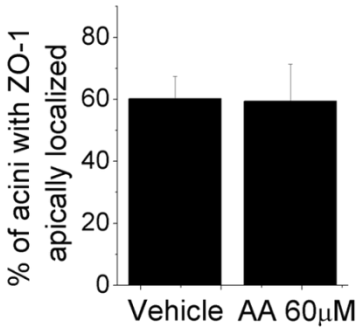

Figure S9. Blind scoring of ZO-1 localization in control and AA-treated acini populations. Acini in control and 60 μM AA-treated groups were fixed and immunolabeled for ZO-1 in three independent experiments (the same ones shown in **Fig. 5**). Here, at least 100 acini were randomly chosen and scored (ZO-1 staining apically localized or not apically localized) per experiment and results were analyzed by Student's t-test.

Supplementary movies:

Movie S1-S3. Three-dimensional images of the same mammary acinus treated with EGTA after 0min (Movie S1), 15min (Movie S2), and 30min (Movie S3). The morphological changes of the mammary acinus were visualized by CARS imaging. Scale bars, 10 μm.